Design of a High Resolution and High Sensitivity Scintillation Crystal Array with Nearly Perfect Light Collection

Craig S. Levin, *Member, IEEE*

Abstract-- **Spatial resolution improvements in Positron Emission Tomography can be achieved by developing detector arrays with finer resolution elements. To maintain high sensitivity and image quality, the challenge is to develop a finely pixellated scintillation crystal array with both high detection efficiency and high light collection. High detection efficiency means the crystals must be relatively long and tightly packed. Extracting a high fraction of the available scintillation light from the ends of long and skinny crystals proves to be very difficult and there is a strong variation with light source depth. The result is inadequate energy resolution. To facilitate light collection, the crystals must be highly polished, which significantly increases costs and complexity. In this paper we examine this poor light collection phenomenon in more detail. We also describe a novel solution we are developing for readout of an array of 1x1x10 mm^3 crystals using avalanche photodiodes (APD). We demonstrate through optical photon tracking simulations that the crystal light collection for this new design is nearly perfect (≥95%) and is independent of the crystal length, width, and surface treatment and origin of the light created.**

I. Introduction

We are developing an ultra-high resolution scintillation detector array for Positron Emission Tomography (PET). Spatial resolution improvements in PET may be achieved by developing a detector array with finer (≤ 2mm wide) resolution elements. However, to realize the desired spatial resolution improvements in reconstructed images, the system sensitivity must also significantly increase to maintain adequate signal-to-noise ratio (S/N) per image resolution element [1]. High resolution is needed for breast and small animal imaging, which are high sensitivity configurations that will help to realize the desired spatial resolution improvements. To maintain high detection sensitivity and good image quality, the challenges are to develop a finely pixellated scintillation crystal array with both high detection efficiency and high light collection. High detection efficiency means the crystals must be relatively long, tightly packed, and cover a relatively large axial field-of-view (FOV).

Unfortunately extracting a high fraction of the available scintillation light from the ends of long and narrow crystals proves to be very difficult due to a poor aspect ratio for light collection. The result is lower S/N, relatively small pulse heights (reduced sensitivity), and inadequate energy resolution (reduced Compton scatter rejection capabilities). This low light extraction also contributes to non-optimized coincidence time resolution. To facilitate light collection, the crystal sides must highly polished, which significantly increases complexity and costs. Furthermore, the light collection efficiency depends upon the origin of the created scintillation light and is worse for points further away from the photodetector. This further degrades energy resolution.

There are several groups developing ultra-high resolution PET systems using scintillation crystals (e.g. [2,3,4]). In these designs either only a fraction of the available scintillation light from 511 keV photon interactions is extracted from the tiny crystals or some sort of compromise between detection efficiency (length), spatial resolution (width), and light collection is made. If optical fibers are used for light readout of crystals as in the system described in [5], even further light loss occurs. Indeed assuming perfectly polished 2x2x10 mm^3 LSO crystals coupled one-to-one to a 2 mm diameter, 10 cm long optical fiber [5], an additional factor > 2 drop in light collection efficiency may be expected and only a very small fraction of the available signal is utilized. Even further light loss occurs without the one-one crystal-fiber coupling [6].

In this paper we describe this poor light collection phenomenon in more detail. We also describe a solution to these problems we are developing that uses avalanche photodiodes (APDs) in a novel light readout configuration for long and narrow crystals. We demonstrate through optical photon tracking Monte Carlo simulations of the scintillation light that with this new design the light extraction from 1 mm wide crystals is nearly perfect (≥95%) and is independent of the length, width, surface treatment of the crystals, and origin of the created light.

II. Theoretical Considerations

A. Spatial resolution potential of PET-motivation for 1 mm detector pixels

To date, no scintillation crystal-based PET system has achieved the fundamental spatial resolution potential inherent to positron imaging. The physical spatial resolution limit is determined by a convolution of three blurring factors: positron range, annihilation photon non-collinearity, and

This work was supported in part by a grant from the Susan G. Komen Breast Cancer Research Foundation.

C.S. Levin is with the VA Medical Center and UCSD School of Medicine, San Diego, CA 92161 USA (telephone: 858-552-7511, e-mail: clevin@ucsd.edu).

0-7803-7324-3/02/$17.00 © 2002 IEEE

intrinsic detector resolution [7]. Figure 1 shows a plot of the calculated spatial resolution for ^{18}F determined by these three factors for various system diameters (or, equivalently, detector separations) as a function of detector element size. In principle, sub-millimeter resolution is attainable with 1 mm detector pixels and ≤ 20 cm detector separation. A gas-filled system [8] has achieved near the spatial resolution potential, but that system has essentially no energy resolving power.

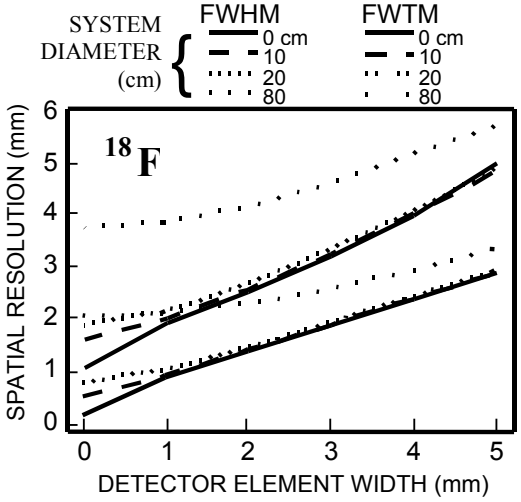

Fig. 1. Calculated point source spatial resolution (FWHM and FWTM) attainable for ^{18}F PET for various system diameters as a function of detector element size. 700μm FWHM resolution is feasible with 1 mm detector elements and ≤20 cm system diameter/detector spacing (Adapted from [6]).

B. Poor light collection from long and narrow crystals

The fraction of the available scintillation light that is collected at the end of a crystal, or *light collection efficiency*, in general depends on the *aspect ratio* (ratio of the crystal readout cross-sectional area *A*, to length *L*). The aspect ratio effects the degree of light absorption and trapping within the crystal and at the surfaces. A high aspect ratio allows optimal light collection. A low aspect ratio, for example would mean that there would be on average a larger number of surfaces (and associated losses) that light rays would encounter before collection and potentially more bulk photon absorption.

An upper limit on light collection efficiency *f*, for a low aspect ratio crystal may be estimated by inspection of Fig. 2 assuming ideal conditions and a poor crystal aspect ratio for light collection. The light loss fraction depends on how much light impinges on the crystal sides at angles less than the critical angle, θ_c for total internal reflection and refracts out of the crystal. This is similar in principle to light transmission into and down a non-clad optical fiber. The solid angle of lost light through one side face, Ω_L is approximately given by:

$$\Omega_L \approx \pi \tan^2\theta_c \approx \pi/n^2, \quad (1)$$

where n = refractive index, θ_c= critical angle for total internal reflection, and we have used Snell's law and expanded the result to first order in $1/n^2$. An estimate for the lower limit on the total light loss fraction may be obtained by multiplying Ω_L by four and dividing by 4π. Thus, the upper limit estimate of the light collection efficiency *f* for low aspect ratio crystals is:

$$f \approx 1 - 1/n^2, \quad (2)$$

which depends only upon *n* and not on crystal details.

According to this expression, higher *n* crystals will on average collect a larger fraction of the available scintillation light. For example, this formula predicts a maximum light collection efficiency of 69 and 78%, respectively for LSO (n=1.82) and BGO (n=2.15) (although, certainly LSO will yield a larger absolute number of photons). In reality, due to imperfect surfaces and external reflectors, and depth dependent effects, the light collection efficiency in general is strongly dependent on the crystal aspect ratio.

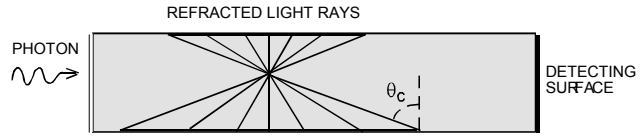

Fig. 2. Depiction of a major mechanism for light loss from poor aspect ratio (long and skinny) crystals. Annihilation photon interaction point is shown near the center; sample light rays emitted from that point are shown. Most of the light impinging on the crystal sides at angles less than the critical angle will exit the crystal or reflect back at similar angles and not be piped down to the small photo-detecting end. Reflectors are on the sides and back.

III. LIGHT COLLECTION SIMULATIONS

Light collection simulations were performed using DETECT [9] which models and tracks the propagation of light photons through the crystal. For these simulations it was assumed that 511 keV interactions produce 10,000 light photons [10] within a volume of 0.001 mm^3 at several points within an LSO crystal. For each light origin, the simulation was performed three times and averaged to improve accuracy. For poor aspect ratio crystals, the light collection efficiency strongly depends upon the light origin within the crystal. The average light collection efficiency for a given crystal configuration was obtained by taking a mean of the simulation results for different source depths weighted with the 511 keV photon interaction probability in LSO at any given depth.

Figure 3 shows the results of Monte Carlo simulations of light collection from the ends of long and narrow scintillation crystals for two different surface conditions. The ideal condition is a perfectly polished crystal with an air gap and a high reflectivity (R=0.98) diffuse reflector on all surfaces except the detecting end. These conditions will promote internal reflection toward the crystal end. The other surface condition is ground (diffuse Lambertian) with the same reflector type. Since in reality it is never possible to achieve surface conditions that promote maximum total internal reflection, under practical experimental conditions the measured light collection efficiency would lie somewhere between the two extremes dictated by the ground and perfectly polished conditions for a given crystal aspect ratio. For example, for a 1x1x10 mm^3 LSO crystal, light collection efficiency will be somewhere between 20 and 60%, and only a fraction of the available detector signal would be realized.

Note that as predicted, due to BGO's higher refractive index its polished light collection efficiency is higher that that of the other crystals. Note also that for these simulations we were concerned mainly with the fraction of light exiting the

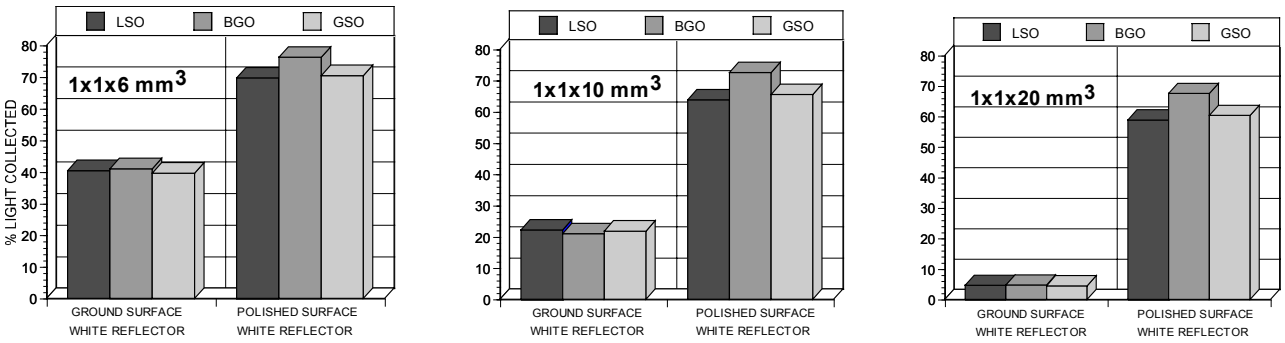

Fig. 3. Average fraction (%) of the available scintillation light collected from the ends of different length and type of 1 mm wide scintillation crystals for two different crystal-surface conditions. Even with the most ideal surface conditions, only a fraction of the light is collected. In reality, the fraction lies somewhere between the two extremes (20-63% for 1x1x10 mm^3 LSO).

crystal and 0.05 mm of optical coupling compound and entering the photodetector. To determine the average total photoelectron signal created by the photodetector, one would multiply the absolute number of photons collected by the quantum efficiency of the device.

IV. How to Obtain Nearly Perfect Light Collection from Long and Narrow Crystals

Figure 4 depicts one proposed readout scheme that facilitates nearly perfect light collection. In such a scheme, 1-D APD "line" arrays with rectangular pixel elements read out light from the long crystal faces. An alternate design could use the position sensitive APD (PSAPD) described in [11]. The main challenges to this scheme are (1) the APD device thickness must be ≤300μm in between crystal planes to maintain a high crystal packing fraction (low dead area) so not to compromise detection sensitivity, and (2) The electronic leads are taken from the bottom of each array as shown. A prototype for the array shown in Fig. 4 has been manufactured using a deep-diffusion process and standard planar silicon device technology [12] and is currently being tested. A very thin device may possibly be achieved by significantly reducing the substrate and/or the wafer thickness. Note that this configuration is not available with photomultiplier tubes (PMTs).

The advantage of collecting the light from the relatively large crystal side faces is that the light crystal aspect ratio (A/L) is significantly increased (10:1 vs. 1:10 for a 1x1x10 mm^3 crystal). Results for light collection simulations of the configuration depicted in Fig. 4 are presented in Fig. 5. The light collection efficiency is nearly perfect (≥95%), independent of crystal length, width and surface conditions, and is also independent of the origin of light creation (compare with Fig. 3). This more complete, non-varying light collection efficiency should lead to more robust detector signals and better energy and perhaps coincident time resolution. The fact that the light collection is independent of surface conditions will also help to significantly reduce crystal array production costs. For example, as long as the crystal faces are flat, freshly saw-cut surfaces may be used.

V. Potential Design Variations

Potential difficulties with tomograph designs comprising many small scintillation crystals are that it is costly and complex to handle many minute crystal elements and align them with their corresponding photodetector element. Any slight misalignment could mean reduced light collection. In addition, fabricating high performance APD arrays that are ≤300μm as depicted in Fig. 4 may be challenging. In Fig. 6, we show alternate solutions comprising sheets of 1 mm thick crystals to replace the discrete crystal planes depicted in Fig. 4. Working with sheets of crystals, perhaps 10x10x1 mm^3, instead of arrays of discrete 1x1x10 mm^3 crystals has the advantage that it is significantly easier and less expensive to cut larger crystal pieces and assemble them into an array. The orientation of the first design (Fig. 6, left) relative to that of incoming photons is the same as for the concept depicted in Fig. 4 and would require ≤300μm APD thickness. Using crystal sheets may ease the difficulties in manufacturing a very thin array since it may be possible to actually completely remove the array substrate and use the crystal instead as backing for mechanical strength to support the silicon wafer. Either line arrays or a PSAPD could be used in this design.

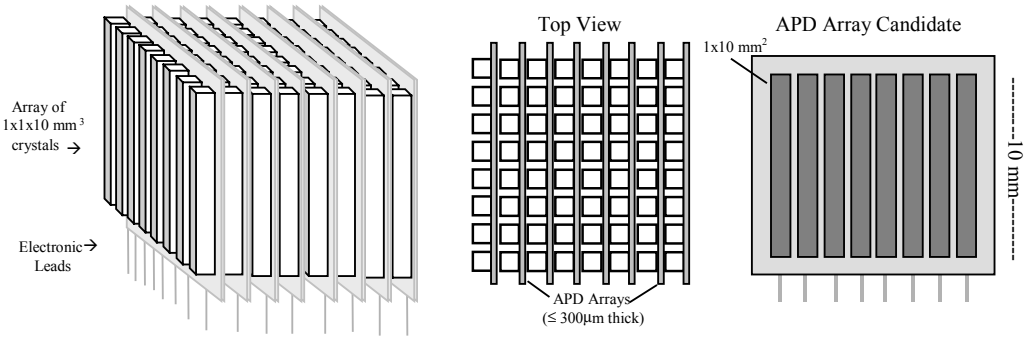

Fig. 4. One proposed readout scheme for an array of 1x1x10 mm^3 crystals using very thin APD arrays that fit compactly between each crystal plane. One candidate APD array design is shown. Each APD element may be segmented lengthwise for depth of interaction information. 511 keV photons enter from top.

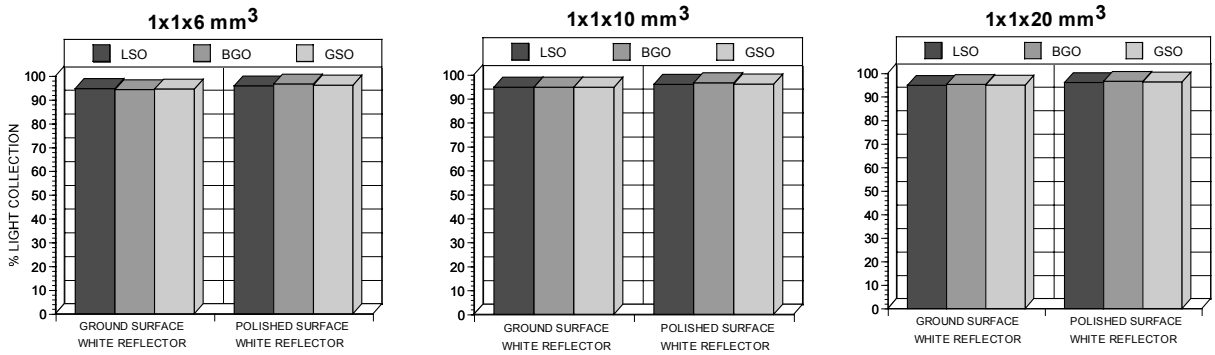

Fig. 5. Nearly perfect (≥95%) light collection that is independent of crystal length, width, and surface conditions, and origin of the scintillation light is possible with the proposed readout. Compare with Figure 3 for the conventional readout. This scheme could help to push the limits of PET spatial resolution (see Figure 1).

The orthogonal configuration (Fig. 6, right) would allow easy depth of interaction determination. This orientation also would allow higher detection sensitivity since incoming photons would not see any detector gaps within the array. This orthogonal orientation also has the advantage that a standard thickness APD array could be used since in this orientation the array would not cause any detection gaps. This orthogonal configuration could be developed by using alternate planes of APD line arrays oriented in the x and y direction on either side of each crystal plane in a "cross-

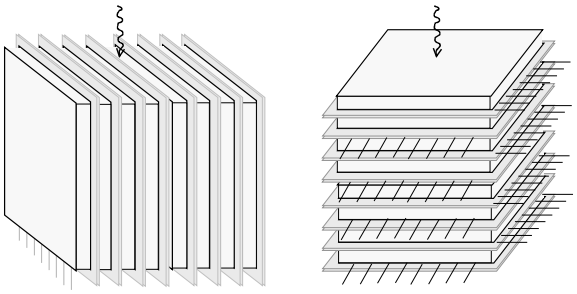

Fig. 6. Alternate detector array concepts involving sheets of crystals instead of arrays of minute discrete crystals. The two different configurations are oriented such that the 511 keV photons enter from the top. APD line arrays used may be as shown in Fig. 4 (right) or as described in [11]. Both arrays would have interaction depth determination capability.

grid" type readout. An interaction point on in any crystal plane would be determined by which cross-strip x and y elements were hit. The orthogonal orientation could also be designed with single PSAPD [11] arrays used in between each crystal plane.

Using crystal sheets instead of minute discrete crystals also has the advantage that the light distribution may involve multiple APD array elements and one may achieve better spatial resolution than the size of the elements by forming an appropriate weighted mean of the various signals involved. A potential disadvantage of this property is that less S/N is available per array element. To study this latter effect we simulated light collection from the large face of a thin, 1x10x10 mm^3 LSO crystal sheet. We simulated point sources at the center and edge of the large area as depicted in Fig. 7. For these central and edge locations, we simulated three different source distances with respect to the photodetector plane as shown: top position corresponded to ~0.1 mm from the top face, the middle position to the crystal center, and bottom to ~0.1 mm from the bottom plane where the photodetector is coupled. Note that the total light collection from the large face was nearly perfect independent of crystal surfaces and source position since this is also a very high aspect ratio (100:1) for light collection.

The calculated light distributions seen at the photodetector plane are shown at the bottom of Fig. 7. Note that for source positions very close to the photodetector plane the exiting light distribution is extremely narrow (see arrows). This is due to the fact that the cones of refracted light ($\theta_i<\theta_c$) subtended from the light origin to the crystal bottom plane and exiting the crystal on first pass, and that which reflects off the top and subsequently exits the bottom surface are narrower for closer distances to the photodetector surface. Thus the base of the detected light cone will also be narrow. The light rays that undergo total internal reflection ($\theta_i>\theta_c$) will for the most part be trapped within the crystal and not contribute significantly to the tails of the distribution.

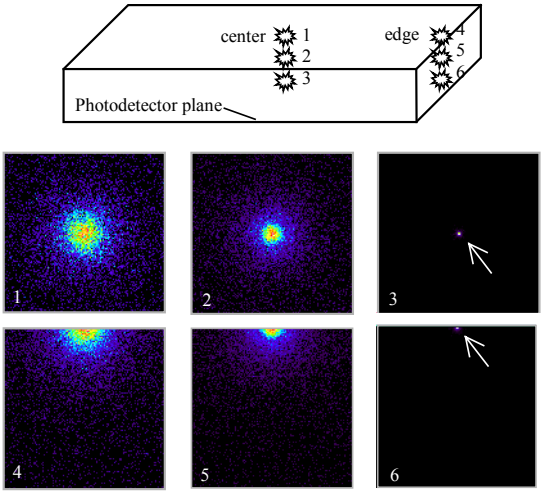

Fig. 7. Top: Configuration for light collection simulations in a 10x10x1 mm^2 LSO crystal for two x-y source locations (center and edge) and three distances z of light pulses from the photodetector face (top, middle, bottom). Bottom: Results of simulations show the light distributions seen at the photodetector plane for the six light source locations. Note for the source positions at the detector plane, the light distribution is extremely narrow.

Light distribution shapes were quantified by fitting horizontal profiles through the center of the light distributions shown in Fig. 7 to a Lorentzian function:

$$f(x)=Aw/[(x-x_0)^2+(w/2)^2)], \quad (3)$$

where x_0 and w respectively, are the peak location and full-width-at-half-maximum (FWHM) of the distribution $f(x)$. The extracted FWHM values and a sample fit (distribution 5 of Fig. 7) are shown in Fig. 8.

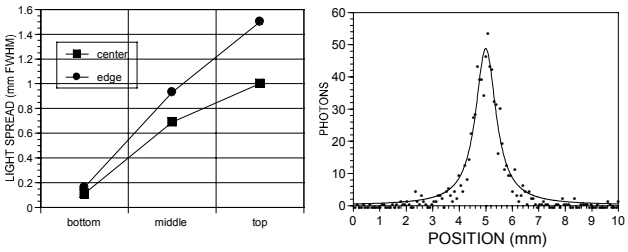

Fig. 8. Left: FWHM of the light distribution profiles shown in Fig. 7. Right: An example fit of a light spread profile to a Lorentzian distribution.

The results in Fig. 8 indicate that the FWHM of the light spread profiles typically do not extend more than 1 mm laterally, with the broadest spread (1.5 mm FWHM) occurring when the light is created 1 mm (the furthest distance possible) from the photodetector face. In all cases at least 90% of the light is contained within 3 mm laterally. Assuming 1 mm wide photodetector array pixels (see Fig. 4) this suggests that only three elements may be necessary to collect a high fraction of the available light. An event could be positioned using a weighted mean on only three signals, avoiding excessive uncorrelated noise propagation, or by selecting the pixel with maximum signal. With a weighted mean approach, resolution would be less than the pixel width.

VI. Discussion and Summary

Sub-millimeter spatial resolution is feasible for PET using ~1 mm detector pixel elements and close-proximity, high sensitivity configurations, such as for small animal or breast imaging. The difficulty of developing a finely pixellated scintillation detector array is that either light collection or 511 keV detection efficiency are necessarily compromised. Over 10,000 light photons are available from a 511 keV photoabsorption in LSO [10]. High light collection efficiency allows optimal detector signals for high sensitivity. Nearly complete light collection is also desirable for optimal energy resolution and maximum Compton scatter rejection capabilities. Energy resolution and Compton scatter rejection capabilities are already non-optimal for very thin crystals since light collection depends on the varying interaction points where light is created within the crystal.

Is Compton scatter a problem for imaging small objects such as laboratory animals? Recent data [13] suggest >30% scatter fraction for a 3-D PET acquisition of a rat-sized object. It is certainly possible to obtain very high resolution images with poor or no energy resolution [8], especially using bone imaging tracers, such as $^{18}F^-$ that have high target-to-background ratio. However, non-optimal energy resolution means non-optimal image contrast and quantitative capabilites, especially for more diffuse tracer concentrations.

We are developing a detector array solution with a goal of nearly complete light collection from 1 mm detector pixels, independent of light source origin. Simulation results suggest this goal is feasible. These properties facilitate maximum use of the available photons for optimal energy resolution. The design will maintain a relatively high crystal length and packing fraction for high detection efficiency. Simulations show that the crystal surfaces are also unimportant which will help to limit the costs of such a design. The high aspect ratio readout configurations suggested are only available to compact semiconductor photodetector arrays, and not PMTs.

We are also investigating the use of thin crystal sheets rather than minute discrete crystals to reduce design complexity, and perhaps improve spatial resolution beyond the readout array pixel size. Two new orthogonal configurations were shown in Fig. 6 with different orientations of the crystal sheets with respect to the incoming photons. Simulation results indicated that there would not be a significant reduction in signal-to-noise ratio since the light distributions created in these thin sheets are very narrow and limited to only a small few photodetector array elements.

VII. References

[1] M.E. Phelps, S.C. Huang, E.J. Hoffman, D. Plummer, R. Carson. An analysis of signal amplification using small detectors in positron emission tomography. *J Comput Assis Tomogr* 1982;6:551-65.

[2] Miyaoka, R.S.; Kohlmyer, S.G.; Lewellen, T.K. Performance characteristics of micro crystal element (MiCE) detectors. *IEEE Trans Nucl Sci*, vol.48, (no.4, pt.2), Aug. 2001. p.1403-7.

[3] Yuan-Chuan Tai, Chatziioannou, A.F., Dahlbom, M., Cherry, S.R. System design for a 1mm^3 resolution animal PET scanner: microPET II. *2000 IEEE Nuclear Science Symposium Conf. Rec*., vol.3, p.21/52.

[4] Seidel, J.; Vaquero, J.J.; Lee, I.J.; Green, M.V. Experimental estimates of the absolute sensitivity of a small animal PET scanner with depth-of-interaction capability. *2000 IEEE Nuclear Science Symposium Conference Record*, (vol.3), p.21/57-9.

[5] S.R. Cherry, Y. Shao, *et al*. Optical fiber readout of scintillator arrays using a multi-channel PMT: a high resolution PET detector for animal imaging. *IEEE Trans. Nucl. Sci*. vol. 43, p. 1932-7.

[6] Y.C. Tai, A. Chatziioannou, *et al*. Performance evaluation of the microPET P4: a PET system dedicated to animal imaging. Physics in Medicine and Biology, vol.46, (no.7), July 2001. p.1845-62.

[7] C.S. Levin, E.J. Hoffman. Calculation of positron range and its effect on the fundamental limit of positron emission tomography system spatial resolution. Phys. Med. Biol. Vol. 44 (1999), pp781-99.

[8] Jeavons, A.P.; Chandler, R.A.; Dettmar, C.A.R. A 3D HIDAC-PET camera with sub-millimetre resolution for imaging small animals. *IEEE Trans Nucl Sci*, vol.46, (no.3, pt.2), June 1999. p.468-73.

[9] G.F. Knoll, T.F. Knoll, T.M. Henderson. Light Collection in Scintillating Detector Composites for Neutron Detection. IEEE Trans Nucl Sci NS-35-1:872-5 (1988).

[10] M. Moszynski, M. Kaputsa, *et al*. Absolute Light Output of Scintillators. *IEEE Trans. Nucl. Sci*. 44(3) (1997) 1052-61.

[11] K.S. Shah, R. Farrel, R.F. Grazioso, E. Karplus. APD Designs for x-ray and gamma-ray imaging. Presented at the 2001 IEEE Nuclear Science Symposium (#NM-3), San Diego CA.

[12] Shah, K.S.; Farrell, R.; Grazioso, R.; Cirignano, L. Large area APDs and monolithic APD arrays. 2000 IEEE Nuclear Science Symposium. Conference Record, vol.1. p.7/22.

[13] C.H. Holdsworth, A. Chatziioannou, R. Leahy, Q. Li, C.S. Levin, M. Janecek, M. Dahlbom, E.J. Hoffman. Data Correction Techniques for Improving the Quantitative Accuracy of MicroPET. *Journal Nuclear Medicine*, Vol. 42, May 2001, 201P. Abstract.